PCCP

Accepted Manuscript

ROYAL SOCIETY OF CHEMISTRY

www.rsc.org/pccp

Theoretical study on the initial stage of Magnesium battery based on V_2O_5 cathode

Bo Zhou,* Hui Shi, Rongfang Cao, Xiaodong Zhang, and Zhenyi Jiang
Institute of Modern Physics, Northwest University,
Xi'an 710069, People's Republic of China

(Dated: July 9, 2014)

Abstract

Several first-principles calculations based on density functional theory have been carried out on the key issues about the magnesium battery with V_2O_5 cathode. This kind of magnesium battery has been reported by D. Aurbach's group in 2013. Our theoretical studies provide explanations to the experimental findings such as higher voltage, slow ion diffusivity and the decrease of the crystallinity. The calculated open circuit voltage of the magnesium battery with V_2O_5 cathode is 3.06 V, which is 0.22 V higher than the lithium battery with the same cathode. The electronic band structure calculations suggest that higher electronic conductivity must be expected in magnesium battery. The elastic constants are obtained, which give the information on the stability of the magnesiated cathode. Further, we have also calculated the diffusion barriers of Li and Mg ions in the cathode using the nudged elastic band method. The hopping barrier of Mg ion is 1.26 eV which is much higher than the Li ion (0.35 eV). The obtained minimum energy paths show the different hopping process in lithium and magnesium battery, which can explain the slow diffusion phenomenon in experiments. The possible pathway between α and δ phases transition is analyzed for the first time, which gives explanation for the reversibility of Mg ion in the V_2O_5 cathode.

Keywords: Magnesium battery, First principle calculation, Elastic properties

---

*Electronic address: zhoubo@nwu.edu.cn

I. INTRODUCTION

There is an urgent need for new rechargeable battery systems which will be made of cheap and environmentally friendly materials suitable for upscaling to large size, *e.g.* for electric vehicles and load leveling application.[?] Magnesium-based rechargeable batteries might be an important future alternative due to the cheaper price and the safety characteristics, as compared with the lithium batteries.[? ?] In 2000, D. Aurbach *et al.* [?] has reported their important achievement in producing the prototype system for rechargeable magnesium batteries, which is made of electrolyte solutions based on Mg organohaloaluminate salts and $Mg_xMo_3S_4$ cathodes.

Meanwhile, the vanadium pentoxide V_2O_5 has attracted a considerable attention due to its outstanding performance in lithium battery applications. There are several experiments of magnesium battery focusing on the vanadium based cathode material such as xerogels, aerogels[?] and microcrystalline V_2O_5[?]. The V_2O_5 gels and their hybrids can exhibit relatively high voltage and capacity upon Mg insertion, but the diffusion of Mg^{2+} ions into the cathode is slow and incomplete.[?] In 2003, D. Aurbach's group has declared their important achievements of producing the nearly full reversible magnesium battery with V_2O_5 film cathode.[?] All these samples can't maintain the crystalline structures after several charging and discharging cycles, which results in poor durability. A proper intercalation mechanism for such materials is still unknown. Several reviews[? ? ?] devoted to Mg cathodes are rather focused on the specific results obtained for various hosts, but not on the mechanism of ionic transport in the cathode.

In the lithium battery side, the experimental studies of V_2O_5 cathode are fruitful. Several $Li_xV_2O_5$ phases have been reported over a large range of temperatures and lithium concentrations. The effect of lithium intercalated into the V_2O_5 frame is fully investigated with experimental and theoretical methods[? ?]. These studies facilitate the research of Mg battery. However, to our knowledge, the theoretical study of Mg atom in the V_2O_5 cathode is scarce, many areas are still untouched yet. We have also noticed that Z. Wang *et al.* have reported their theoretical results on single-layer V_2O_5 as a promising cathode for Mg ion battery.[?] The diffusion barrier and the bind energy of Mg-V_2O_5 system has been given. The complexities in the electrochemical behavior of Mg batteries has not been fully pointed out in the available scientific studies. In this work, we present several first principle calculations on the open circuit voltage and cations diffusing process. Efforts have been made to figure out the mechanism of Mg ions diffusion in the V_2O_5 cathode and the difference from the lithium battery applications. We are aiming to gain information necessary for the future design and optimization of the synthesis of the V_2O_5 bronzes with higher capacity.

II. METHODOLOGY

All the calculations are performed within theoretical framework of density function theory (DFT) as implemented in the Vienna *ab initio* simulation package (VASP)[**?**] with a plane wave basis set. The projector augmented wave (PAW) method is employed to describe the electron-ion interaction. The generalized gradient approximation (GGA) using the Perdew-Burke-Ernzerhof (PBE) functional is used to describe the electron exchange-correlation.[**?**] The plane wave basis set cutoff energy is 600 eV for each solid. The Brillouin-zone sampling grid is Γ centered $6\times6\times6$ homogeneously distributed grid. The criterion for the convergence of the electronic self-consistency cycles is 10^{-8} eV. Ionic coordinates are fully relaxed until the residual of forces are less than 10^{-4} eV/$\AA^{-1}$ and pressure is less than 0.004 GPa. The elastic tensor is determined by performing six finite distortions of the lattice and deriving the elastic constants from the strain-stress relationship [**?**]. The final elastic moduli includes both the contributions from distortions with rigid ions and the contributions from the ionic relaxations.

Further, we have carried out the rotationally invariant GGA+U calculation as implemented in VASP. The effective on-site Coulomb interaction parameter of U is 4.0 eV as suggested by other prior work[**?**]. For comparison purpose, the vdW-DF2 functional of Langreth and Lundqvist groups [**?**] have also been used to get the electronic band structures.

Energy barriers of the diffusion process are calculated using the nudged elastic band (NEB) method.[**?**] The NEB is an efficient method to determine the minimum energy path (MEP) and saddle points between the given initial and final positions. A chain of images (eight in the present calculations) are initially determined through linear interpolation from the initial and final configurations. The minimum energy path is obtained, after optimization of all degrees of freedom of each structure involving the images interactions as elastic band forces.

III. RESULTS

A. STRUCTURES

Several polymorphs of V_2O_5 are involved in this paper. The structure of the bulk V_2O_5 is called α-V_2O_5.[?] The relaxed LiV_2O_5 (named as ϵ-LiV_2O_5)[?] is the structure of $Li_xV_2O_5$ system at low lithium concentration with very little structural distortion from the bulk oxide. The α phase and the ϵ phase of $Li_xV_2O_5$ are stable at temperatures below 400 °C with low lithium concentration ($x \leq 0.13$ for α phase and $0.3 \leq x \leq 0.8$ for ϵ phase).[?] At the initial stage of the discharging process of magnesium battery, only a small amount of Mg ions has intercalated into the cathode, and the geometry of cathode material has small changes. Experiments [? ?] has also confirmed that the V_2O_5 cathode at the initial stage of the discharge process forms the similar structure as α-V_2O_5. Since no crystallographic data for $Mg_xV_2O_5$ at each stage of the battery charging and discharging process have been reported, we infer the position of Mg atoms by analogy with Li atoms in $Li_xV_2O_5$ suggested by lithium battery studies. So we name it as α-MgV_2O_5 distinct from the ordinary magnesium vanadate. All these three structures are orthorhombic crystal with the same space group *Pmmn* (No. 59) as shown in Figure 1(a). The ordinary MgV_2O_5 crystallizes in the orthorhombic base-centered space group *Cmnm* (No. 63) which has been intensively studied as low-dimensional spin ladder system.[?] The δ-$Li_xV_2O_5$ structure determined from powder pattern neutron diffraction showed similar structure with MgV_2O_5.[?] The ordinary MgV_2O_5 can be considered as Mg ion in δ-V_2O_5. In the intercalation reaction, $Mg_xV_2O_5$ system can adopt many phases depending on temperature and concentration x, which may even more complex than the $Li_xV_2O_5$ system.[?] Only α and δ phase are considered in this paper. Both the α-type structures has the same crystallographic arrangements which are different from the δ-type (ordinary MgV_2O_5 and δ-V_2O_5).

The structures from the theoretical optimization and the experiments are listed in Table 1. The overestimation of c parameter (7.5 %) in pure V_2O_5 can attribute to the limitation of the DFT method for modeling Van der Waals interaction. In α-type structures, the Li and Mg ion is located at the Wyckoff position *2b* which has the same site symmetry *mm2* as the *4c* in δ-type structures. The intercalated Li and Mg ions eliminate the effect of *Van der Waals* force, which makes the optimized geometry quite close to the experimental measurements. Large deviation occurs for the α phase of MgV_2O_2 which attributes to the lack of large pure sample. The α-MgV_2O_2 is metastable and only exists in low concentration, according to our following study. From our results, the c axis of V_2O_5 frame increases when the Li/Mg ions are intercalated. This tendency is the same as the XRD refinement results from P. Novak [**?**]. The ϵ-MV_2O_5 (M=Li, Mg) also shows a steady expansion of the c lattice parameter as the increased concentration of ions between the V_2O_5 layers.

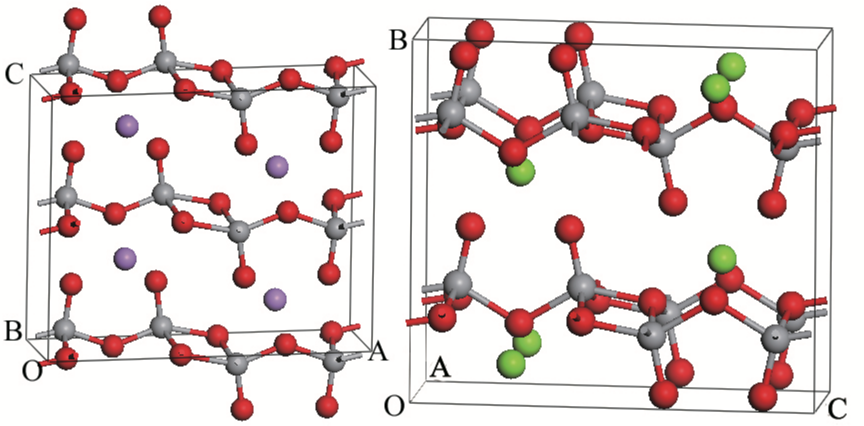

FIG. 1: The crystal structure of the α type (a) and δ type V_2O_5 (b). The red ion is oxygen and the gray is the vanadium. The other color represents the intercalated ion, Li or Mg in our paper. For comparison, α type V_2O_5 (a) is 1×1×2 supercell and δ type V_2O_5 is described in the conventional cell.

B. Open circle voltage

Firstly we compare the open circuit voltage of both two kinds of battery. The open circuit voltage (OCV) is defined as the difference of the chemical potential between the two electrodes.[**?**] We use the following equation:

$$V(x) = (\mu^{cathode}(x) - \mu^{anode})/zF \tag{1}$$

Where F is the Faraday constant and z is the charge (in electrons) transported in electrolyte. The chemical potential is approximated by the internal energy while neglecting the entropy and temperature contributions. The metallic lithium internal energy is calculated from the body-centered cubic structure, while the magnesium one is obtained from hexagonal

TABLE I: Comparison of theoretical and experimental lattice parameters. Values in column 2, 3, 4 and 5 are in units of Å. The percent deviations are in parentheses.

α-V_2O_5	exp.[a]	PBE	VDW-DF2	GGA+U
a	11.512	11.563 (0.4%)	11.860 (3.0%)	11.483 (-0.3%)
b	3.564	3.565 (0.03%)	3.585 (0.6%)	3.637 (2.0%)
c	4.368	4.696 (7.5%)	4.478(2.5%)	4.798 (9.8%)
ϵ-LiV_2O_5	exp.[b]			
a	11.355	11.362(0.6%)	11.511(1.4%)	11.474(1.0%)
b	3.573	3.573 (0.0%)	3.610(1.0%)	3.627(1.5%)
c	4.655	4.721 (1.4%)	4.712(1.2%)	4.675(0.4%)
α-MgV_2O_5	exp. [c]			
a	11.508	11.615 (0.9%)	11.799 (2.4%)	11.599 (0.8%)
b	3.568	3.301 (-7.5%)	3.359 (-5.9%)	3.396 (-4.8%)
c	4.372	4.810 (9.1%)	4.854 (11.0%)	4.808 (10.0%)
MgV_2O_5	exp. [d]			
a	3.693	3.761 (1.8%)	3.802(3.0%)	3.801(2.9%)
b	9.958	10.029 (0.7%)	10.096(1.4%)	9.983(0.3%)
c	11.010	10.796 (-1.9%)	10.953 (-0.5%)	10.920(-0.8%)

[a] Ref. [**?**]
[b] Ref. [**?**]
[c] Ref. [**?**]
[d] Ref. [**?**]

close-packed structure. The full metal anode is considered. $\mu^{cathode}(x)$ is taken as the energy difference between the lithiated/magnesiated compound and the pure cathode. In the lithium battery case, we use the energy of ϵ-LiV_2O_5 which is formed at low concentration of x ($0.3 < x < 0.8$) with an irreversible phase transition. As suggested by the work of P. Novak[**?**], the crystallographic data of α-MgV_2O_5 is taken as the "final" state of the cathode after Mg ion intercalation. The OCV of both Li and Mg battery with the V_2O_5 cathode are calculated within the same theoretical level. The OCV of the lithium cell is 2.84 V, which is consistent with the theoretical study of J. S. Braithwaite *et al.*[**?**] This value is

TABLE II: The calculated open circle voltage from different methods. All values are in Volt.

	PBE	GGA+U	VDW-DF2
Li	2.84	2.49	3.25
Mg	3.06	2.82	3.60

smaller than the maximum of the experiment voltage window 2.0-4.0 V, since the energy of ϵ-LiV_2O_5 used in equation 1 is not the final phases of the discharge process. The OCV of the Mg battery is 3.06 V. Our calculations indicate that the voltage expected with a Mg battery is about 0.22 V higher than that of a Li battery with the same V_2O_5 cathode. No explicit OCV value of Mg battery has been reported yet. From the comparison of cyclic voltammograms for Li and Mg intercalation processes which has been reported by E. Levi[**?**], P. Novk's[**?**] and D. Aurch[**?**], the peak of redox potential of Mg-V_2O_5 system is 0.2 - 0.3 V higher than the Li-V_2O_5 system.

Further, we have calculated the OCV with the GGA+U method and vdW-DF2 functional as shown in Table 2. The vdW-DF2 results overestimate the OCV and the difference is 0.35 V. GGA+U method gives more reasonable result which shows a 0.33 V difference. Anyway, the results from PBE method are acceptable and the following results are based on it.

C. Band structures

Secondly, we has calculated the band structures of pure α-V_2O_5, ϵ-LiV_2O_5, α-MgV_2O_5 and ordinary MgV_2O_5 as shown in Figure 2. Band structures give information on the electronic conductivity of magnesiated V_2O_5 cathode. The fine details of the band structure of α-V_2O_5 (Fig. 2(a)) agree well with previous study. The direct gap of V_2O_5 is 2.17 eV and the indirect gap is 1.87 eV, which is almost the same with our previous study.[**?**] From Fig. 2(b), The Li atom is fully ionized in cathode and donates its electron to the host bands without much affecting them. It should also be noticed that the relaxation after lithium intercalation makes the band structure of the V_2O_5 frame change from indirect gap to direct gap, while the gap increases to 2.32 eV. The width of the split bands increases from 0.53 eV to 0.94 eV. The α-MgV_2O_5 bands has a metallic character as shown in Figure 2(c). The split bands become wider and merge to the conduct bands. The incorporation of the magnesium atom makes the band gap value slightly change from 1.87 eV to 1.82 eV. From Figure 2(d), the band structure of ordinary MgV_2O_5 poses a very small band gap 0.02 eV, which is consistent with results from J. Spitaler *et al.*[**?**] The band gap of the original V_2O_5 bronze changes from indirect gap to the direct gap. These calculations indicate the electronic conductivity will increase as the intercalation of the Mg ions. There isn't electronic conductivity issues for the V_2O_5 cathode.

We also notice that ”The change of the electrode color upon the electrochemical process from yellow to faint green” in Ref. [**? ?**] which indicates the energy gap of the magnesiated cathode increases from about 2.14 eV (yellow) to 2.34 eV(green)[**?**]. This phenomenon has also been reported by several experimental studies with slightly different descriptions. These two energy values are nearly equal to the direct band gap of α-V_2O_5 and ϵ-LiV_2O_5 respectively. That is coincidence in consideration of the characteristic of DFT theory and the overestimated c lattice parameter. The conversion from indirect gap to direct gap should also be noted. We can't distinguish that the reason for the color changing is whether from the band gap enlargement or from the indirect-direct changes induced by the ions intercalation.

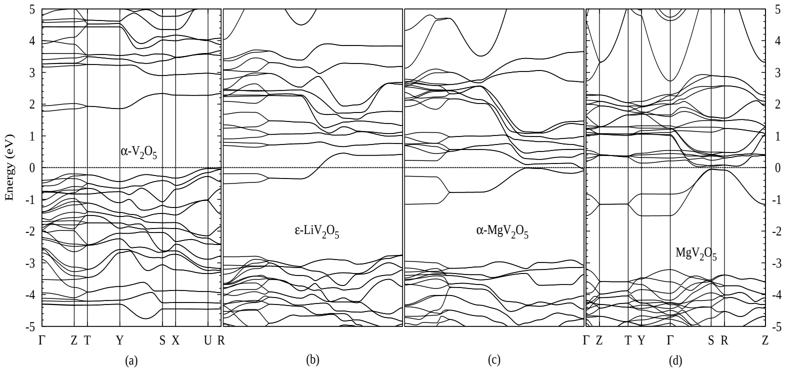

FIG. 2: The electronic band structures of pure α-V_2O_5(a), ϵ-LiV_2O_5(b), α-MgV_2O_5(c) and ordinary MgV_2O_5(d).

D. Stability of the α-MgV_2O_5

The elastic constants are important parameters to describe the response to an applied macroscopic stress, which also give information on mechanical hardness and stability of the

TABLE III: Elastic constants of the α-V_2O_5, ϵ-LiV_2O_5, α-MgV_2O_5, δ-V_2O_5 and ordinary MgV_2O_5 calculated within finite difference method. The Voigt notation replaces xx→1, yy→2, zz→3, zy(yz)→4, xz (zx)→5 and xy (yz)→6. All values are in units of GPa.

	V_2O_5	ϵ-LiV_2O_5	α-MgV_2O_5	δ-V_2O_5	MgV_2O_5
c_{11}	159.5	181.3	266.2	172.9	201.4
c_{22}	213.1	164.9	147.1	5.7	138.8
c_{33}	14.9	51.0	139.4	134.5	142.4
c_{12}	107.3	89.5	91.7	1.6	78.8
c_{13}	21.4	18.9	45.4	92.5	122.9
c_{23}	12.4	27.2	42.2	5.0	55.2
c_{44}	13.6	-46.5	-4.9	8.7	33.9
c_{55}	19.4	11.2	15.0	35.7	11.9
c_{66}	40.6	50.2	30.2	-3.5	11.1

material. The orthorhombic lattice has nine independent elements in the elastic matrix according to the D_{2h} symmetry. All the nine elastic constants of these four structures are obtained within the density functional theory as listed in Table 3. The elastic constants of δ-V_2O_5 without any ion intercalation has also been calculated for comparison purpose. It should be noticed that the definitions of the elastic constants of α-type structures (α-V_2O_5, ϵ-V_2O_5 and α-MgV_2O_5) are the same while the δ-type structures (δ-V_2O_5 and MgV_2O_5) are different as shown in Figure 1. The Voigt notation are adopted with the relation to the crystal axis xx→1, yy→2, zz→3, zy(yz)→4, xz (zx)→5 and xy (yz)→6. Mechanical stability leads to restrictions on the elastic constants, which for orthorhombic crystal are[**?**]

$$(c_{11} + c_{22} - 2c_{12}) > 0, \tag{2a}$$

$$(c_{11} + c_{33} - 2c_{13}) > 0, \tag{2b}$$

$$(c_{22} + c_{33} - 2c_{23}) > 0, \tag{2c}$$

$$c_{11} > 0, c_{22} > 0, c_{33} > 0, \tag{2d}$$

$$c_{44} > 0, c_{55} > 0, c_{66} > 0, \tag{2e}$$

$$(c_{11} + c_{22} + c_{33} + 2c_{12} + 2c_{13} + 2c_{23}) > 0 \tag{2f}$$

From our results, it is obvious that α-V_2O_5 is more soft (easier to expand or compress) in the direction perpendicular to the layers and vulnerable to the shear distortion. The elastic constants of α-V_2O_5 in Table 3 satisfy all of these conditions in Equation 2. And so does the ordinary MgV_2O_5 as expected. Compared to other directions, the value of C_{33} is a better estimate of the bulk modulus of the system. Based on the results, the intercalation of Mg ion makes the sample stiffer, specially in the direction perpendicular to the $[V_2O_5]_n$ layers. The intercalation of lithium ion hasn't dramatic change in the cathode mechanical strength. All the elastic constants of ϵ-LiV_2O_5 are much close to those of α-V_2O_5 except for the C_{44} component. The Voigt notation of C_{44} indicates the response of the stress σ_{xz} to the strain incurred by the deformation δ_{xz}. The minus value of C_{44} means the structure are unstable and unable to maintain its structure while encountering shear distortion in yz plane (bc plane in orthorhombic cell). The instability to the yz plane distortion also exists in the α-MgV_2O_5. The pure δ-V_2O_5 has instability in the xy plane. From Figure 1, these two instabilities are the same despite of the different crystallographic arrangement used. The α phase and δ phase are connected via the distortion of the yz plane (in α phase) or xy plane (δ phase). Meanwhile large variation of the elastic constants may cause cracks in the cathode samples which has been observed by serval experiments.[**?**]

E. Diffusivity

High ion diffusivity is important to satisfy the current-density requirements. The nudged elastic band method is an efficient method to find the minimum energy diffusion path between the given initial and final states. As shown in Figure 1, α-V_2O_5 bronze has layer structure and Li atoms occupy the center of four VO_6 octahedrons running parallel to the B axis of the orthorhombic lattice. This kind of crystal structure provides three spatial diffusion tunnels, one running parallel to the B axis (the shortest lattice parameter), the other two through the $[V_2O_5]_n$ plane. From our previous results,[**?**] the diffusion of Li ions is one-dimension hopping process. The energy barrier for the diffusion along the B axis is quite small (0.35 eV) and the energy barriers along the other two directions are much higher (1.88 eV along the A axis, 1.69 eV along the C axis) which prohibits the diffusion occuring along these two directions. The host material is typically little affected by the intercalation of lithium. Lack of phase change enables all the lithium to be removed reversibly, without the need for energy wastage associated with the nucleation of new phases or the sluggish reactions when massive rearrangement of the host must occur as the lithium concentration is high. As shown in Figure 3(a), the MEP of lithium ion diffusing in α-V_2O_5 poses the single peak configuration.

We have calculated the Mg ion diffusion in α-V_2O_5 with same diffusion pattern. The energy barrier we obtained (Figure 3(b)) is 1.26 eV much higher than the Li case. The Mg ion diffusing in the δ-V_2O_5 has also been calculated within the same theoretical level (Figure 3(c)). The MEP of the migration of Mg ion in the δ-V_2O_5 shows double peak configuration, and the highest barrier is 1.38 eV and the energy barrier of intermediate state is 0.8 eV. The scheme of the path of Mg in δ-V_2O_5 has shown in Figure 4. In the calculation of Mg in α-V_2O_5, the lattice parameters are fixed and only the Mg ions and nearby oxygen ions are allowed to move. Until now, only the Chevrel phases, $M_xMo_6T_8$ (M=metal, T=S, Se) in their usual microcrystalline state, allows for fast and reversible Mg intercalation at ambient temperatures.[**?**] In 2013, the nearly fully reversible Mg battery based on V_2O_5 film has been developed by D. Aurbach's group.[**?**] But the charging and discharging rate isn't fast enough. The slow Mg diffusion was generally assigned to high migration barrier which causes by the strong Mg interactions with the anions and the cations of the hosts and the polarization effect of Mg^{2+} cations with a high charge radius ratio.

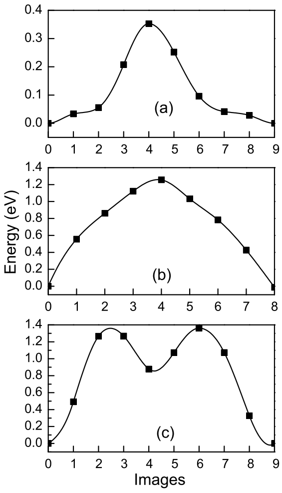

FIG. 3: The minimum energy paths of the diffusion of Li (a) and Mg (b) ion in α-V_2O_5 cathode and in δ-V_2O_5 cathode(c)

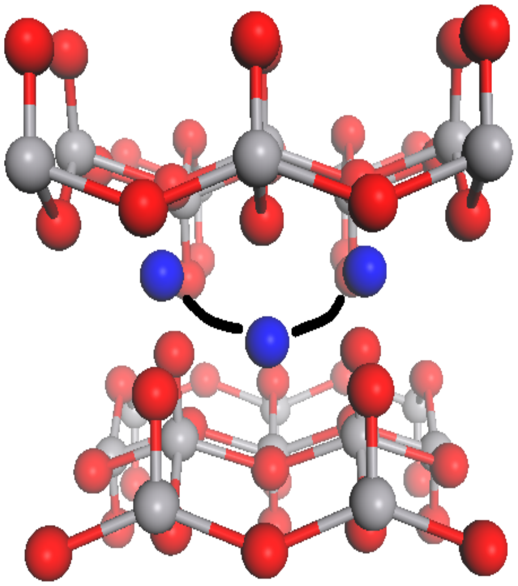

FIG. 4: Schematic diagram of the minimum energy pathway of Mg in δ-V_2O_5 cathode

The magnesium-ion diffusivity can be estimated from the activation energy according to the Arrhenius equation.

$$D = d^2\nu^* exp(-E_{act}/k_bT)$$

where k_B is the Boltzmann constant and T is the temperature. d is the hopping distance and ν^* is the attempt frequency. The hopping distance in MgV_2O_5 is approximately 3.5 Å. The frequency ν^* is about 3×10^{13} Hz as taken from theoretical work of J. Spitaler el.[**?**]. If 0.8 eV is taken as the average barrier, the diffusivity of Mg in V_2O_5 cathode can be approximated to be $1.34 \times 10^{-15} cm^2 s^{-1}$ at 300 K, while the Li diffusivity is about $4.85 \times 10^{-8} cm^2 s^{-1}$ with the same parameters except the energy barrier. Apparently, the Mg ions diffusivity is too low for batteries.

F. Phase transition

The δ phase of V_2O_5 is always described as $[V_2O_5]_n$ layers alternately displaced a/2 (a is the lattice parameter of δ-V_2O_5) along the [100] direction as shown in Figure 1(b). The corresponding b parameter is then doubled and the space group becomes *Cmcm* (with *Cmc2* and *C2cm* as other possibilities). The main transition pathway between the α and δ phases is through the displacement of the $[V_2O_5]_n$ layers. If we take a closer look at the difference between the α and δ type structures, another transformation path can be found. As shown in Figure 5, the rotation of the $[V_2O_5]_n$ layer along the x axis (a axis of the lattice) can also lead to the δ phase. This transition path is consistent with the shear distortion suggested by the elastic constants study in our previous section. The variance of lattice is from atom-fixed view of this transition and the rotation of the $[V_2O_5]_n$ is from the cell-fixed view. The rotation of the layers can take any angle from 0 to about 22° (arctan(0.5b/c), b and c are lattice parameters of α-V_2O_5) as shown in Figure 6. This rotation angle is concerned with concentration of magnesium ions. Partial transformation occurs at very low concentration. At high Mg concentration, the rotation angle will reach 22°, all the α phase will change to the δ phase. Just from the structural view, this transformation is a barrierless reaction. The magnesium concentration is the critical factor to control this transition.

In our current theoretical level, the energy difference between the α-V_2O_5 (-115.98 eV) and δ-V_2O_5 (-115.81 eV) is 0.17 eV. It is a quite small energy difference compared to our previous study. The total energy of α-MgV_2O_5 (-125.10 eV) is about 0.96 eV higher than ordinary MgV_2O_5 (-126.06 eV) within our theoretical level. To simulate this transition, we have tried the nudged elastic method involving both atomic and unit cell degrees of freedom.[**?**] Convergence problem has been met in the calculating of α-MgV_2O_5 to ordinary MgV_2O_5. Very large supercell is needed to obtain well converged and smooth MEP curve, which we can't afford. We take another method. Ten images are prepared with equally displaced of the $[V_2O_5]_n$ layers from the original α-V_2O_5. Then, We fully optimize the cell parameter and the ionic position of each images only keep the relative positions in y direction fixed. From our results as shown in Figure 7, this potential curves show clear barrierless character.

From our results, the diffusion in the α-V_2O_5 are quite slow as compared to the Li ions because of very high hopping barrier. The barrierless transition of the α-V_2O_5 indicates that the formation of δ phase MgV_2O_5 accompanying with the intercalation of Mg ions. From our NEB calculation, the formation of MgV_2O_5 (δ phase) increase the hopping barrier for the Mg ions. As consider the large potential well as the MgV_2O_5 related to the α-V_2O_5 and the stability of the pure MgV_2O_5, The transition is very harmful for the battery. How to suppress this transition should be paid more attention to.

J. P. Pereira-Ramos's early work[**?**] has showed that the electrochemical reduction of V_2O_5 in $Mg(ClO_4)_2$ or $Mg(CF_3SO_3)_2$ solutions at 150°C leads to the formation of $Mg_xV_2O_5$, and this process is found to be fairly reversible. The stoichiometric ratio of magnesium ions inserted into V_2O_5 can reach up to about x=0.5. The very important effect of the temperature hasn't been taken into account in our current theoretical study. From the electronic band structure calculation, the electronic conductivity of V_2O_5 cathode is also very sensitive to the temperature. The molecular dynamics study of the Mg ion diffusion in the V_2O_5 cathode with temperature effect involved is undertaken.

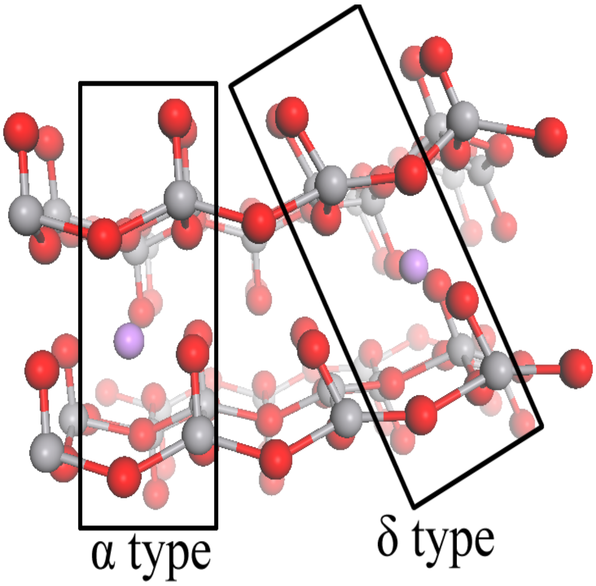

FIG. 5: Schematic diagram of α-V_2O_5 and δ-V_2O_5 transformation

IV. SUMMARY

In summary, our first principles calculations give that the magnesium battery with crystalline V_2O_5 electrode should have an open circuit voltage 3.06 V which is 0.22 V higher than the lithium battery with the same cathode material. The electronic band structures of pure α-V_2O_5, ϵ-LiV_2O_5, α-MgV_2O_5 and ordinary MgV_2O_5 has been calculated, which shows the effect of the inserted ion on the the cathode. The metallic band structure of α-MgV_2O_5 and the very small band gap of ordinary MgV_2O_5 suggest high electronic conductivity. The relaxation after lithium and magnesium intercalation makes the band structure of the V_2O_5 frame change from indirect gap to direct gap. Potential reason for the color changing phenomena in experiments has been discussed.

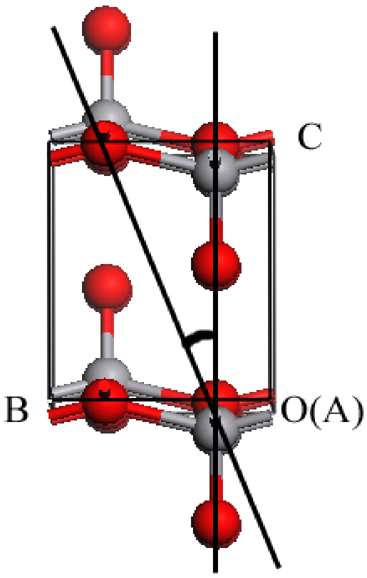

FIG. 6: The rotation angle of the transition from α-V_2O_5 to δ-V_2O_5, which is equal to $\arctan(0.5b/c)$ (b and c are the lattice parameters of α-V_2O_5).

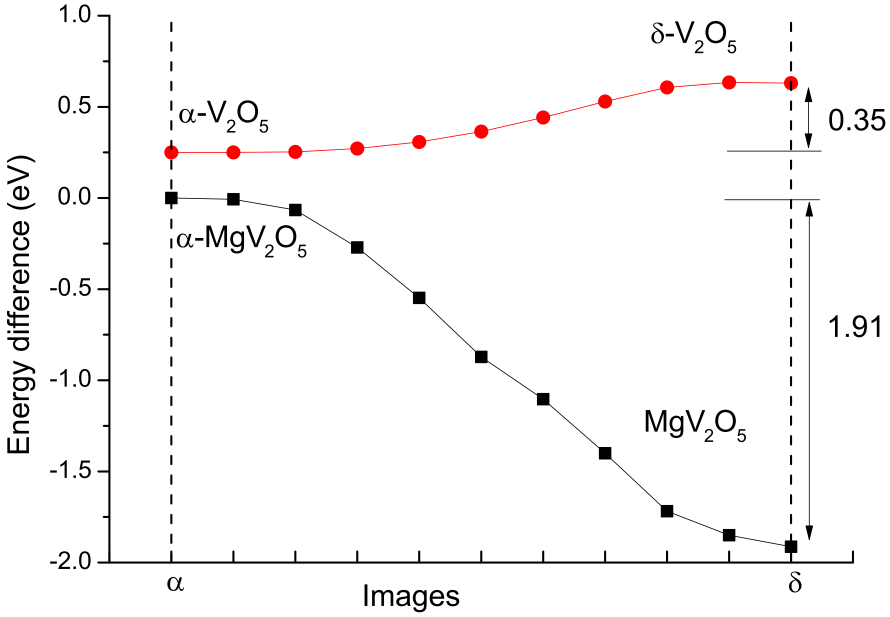

FIG. 7: The potential energy curve of the transition from α-V_2O_5 to δ-V_2O_5(a) and from α-MgV_2O_5 to ordinary MgV_2O_5(b). The 1×2×1 supercells of α-V_2O_5 and α-MgV_2O_5 are used.

Li diffusion in α-V_2O_5 is one dimensional hopping process with energy barrier 0.35 eV, and the potential of this path shows single peak configuration. While the Mg in this cathode have a much higher barrier 1.26 eV with the same hopping pattern. We has also calculated the Mg hopping barrier in δ-V_2O_5 which has a double-peak potential energy path and 0.81 eV barriers. Our hopping barrier calculation can explain the slow diffusion of Mg ion in the V_2O_5 cathode.

Elastic constants of lithiated and magnesiated cathode has been calculated. The intercalation of Mg ion makes the cathode stiff, also makes the cathode vulnerable to shear distortion. The important phase transition of the α and the δ phases has been discussed. Our results shows this kind of phase transition is an barrierless process with the rotation of the $[V_2O_5]_n$ layers.

Under the conditions expected in a real Mg battery, the insertion of Mg^{2+} into V_2O_5 would be a very complex process and the competition between Mg^{2+} ions diffusion and the phase transforming of the bronze may be the source of the application problems. The influence of the temperature on the battery should be fully taken into consideration, and the further work is being undertaken.

Acknowledgments

The authors acknowledge the support of the National Science Foundation of China under Grants No.11104219.

[1] Armstrong, A. R.; Lyness, C.; Panchmatia, P. M.; Islam M. S.; Bruce, P. G. The lithium intercalation process in the low-voltage lithium battery anode $Li_{1+x}V_{1-x}O_2$. *Nature Mater.* **2011**, 10, 223-229.

[2] Novk, P.; Imhof, R.; Hass, O.; Magnesium insertion electrodes for rechargeable nonaqueous batteries - a competitive alternative to lithium? *Electrochim. Acta* **1999**, 45, 351-367.

[3] Levi, E.; Gofer, Y.; Aurbach, D.; On the Way to Rechargeable Mg Batteries: The Challenge of New Cathode Materials. *Chem. Mater.* **2010**, 22, 860-868.

[4] Aurbach, D.; Lu, Z.; Schechter, A.; Gofer, Y.; Gizbar, H.; Turgeman, R.; Cohen, Y. ; Moshkovich, M.; Levi, E.; Prototype systems for rechargeable magnesium batteries. *Nature*,

2000, 407, 724-727.

[5] Le, D. B.; Passerini, S.; Coustier, F.; Guo, J.; Soderstrom, T. ; Owens, B. B.; Smyrl, W. H. Intercalation of Polyvalent Cations into V_2O_5 Aerogels. *Chem. Mater.* **1998**, 10, 682-684.

[6] Shklover, V.; Haibach, T.; Ried, F.; Nesper, R.; Novk, P.; Crystal Structure of the Product of Mg^{2+} Insertion into V_2O_5 Single Crystals. *J. Solid State Chem.* **1996**, 123, 317-323.

[7] Tang, P. E.; Sakamoto, J. S.; Baudrin, E.; Dunn, B.; V_2O_5 aerogel as a versatile host for metal ions. *J. Non-Cryst. Solids,* **2004**, 350, 67-72.

[8] Gershinsky, G.; Yoo, H. D.; Gofer, Y.; Aurbach, D.; Electrochemical and Spectroscopic Analysis of Mg^{2+} Intercalation into Thin Film Electrodes of Layered Oxides: V_2O_5 and MoO_3. *Langmuir* **2013**, 29, 10964-10972.

[9] Gregory, T. D.; Hoffman, R. J.; Winterton, R. C.; Nonaqueous Electrochemistry of Magnesium: Applications to Energy Storage. *J. Electrochem. Soc.* **1990**, 137, 775-780.

[10] Bruce, P. G.; Krok, F.; Nowinski, J.; Gibson, V. C.; Tavakkoli, K.; Chemical Intercalation of Magnesium into Solid Hosts. *J. Mater. Chem. 1991*, 1, 705-706.

[11] Braithwaite, J. S. ; Catlow, C. R. A.; Gale, J. D.; Harding, J. H.; Lithium Intercalation into Vanadium Pentoxide: a Theoretical Study. *Chem. Mater.* **1999**, 11, 1990-1998.

[12] Rocquefelte, X.; Boucher, F.; Gressier, P.; Ouvrard, G.; First-Principle Study of the Intercalation Process in the $Li_xV_2O_5$ System. *Chem. Mater.* **2003**, 15, 1812-1819.

[13] Wang, Z.; Su Q.; Deng, H.; Single-layered V_2O_5 a promising cathode material for rechargeable Li and Mg ion batteries: an *ab initio* study. *Phys. Chem. Chem. Phys.* **2013** 15, 8705-8709.

[14] Kresse, G.; Furthmuller, J.; Efficiency of ab-initio total energy calculations for metals and semiconductors using a plane-wave basis set. *Comput. Mater. Sci.* **1996**, 6, 15-50.

[15] Perdew, J.P.; Burke, K.; Ernzerhof, M.; Generalized Gradient Approximation Made Simple. *Phys. Rev. Lett.* **1996**, 77, 3865-3868.

[16] Page, Y. Le; Saxe, P.; Symmetry-general least-squares extraction of elastic data for strained materials from ab initio calculations of stress. *Phys. Rev. B* **2002**, 65, 104104.

[17] Scanlon D. O.; Walsh, A.; Morgan, B. J.; Watson, G. W.; An ab initio Study of Reduction of V2O5 through the Formation of Oxygen Vacancies and Li Intercalation. *J. Phys. Chem. C* **2008**,112, 9903-9911

[18] Klimes, J.; Bowler D. R.; Michaelides, A.; Van der Waals density functionals applied to solids *Phys. Rev. B* **2011**, 83,195131

[19] Henkelman, G.; Uberuaga, B. P.; Jonsson, H.; A climbing image nudged elastic band method for finding saddle points and minimum energy paths. *J. Chem. Phys.* **2000**, 113, 9901-9904.

[20] Enjalbert, R.; Galy, J.; A Refinement of the structure of V_2O_5 *Acta Cryst.* **1986**, C42, 1467-1469.

[21] Satto, C.; Sciau, P.; Dooryhee, E.; Galy, J.; Millet, P.; The $\delta \rightarrow \epsilon \rightarrow \gamma$ "High Temperature Phase" Transitions Evidenced by Synchrotron X-Ray Powder Diffraction Analysis. *J. Solid State Chem.* **1999**, 146, 103-109.

[22] Novk, P.; Shklover, V.; Nesper, R.; Magnesium Insertion in Vanadium Oxides: A Structural Study. *Z. Phys. Chem.* **1994**, 185, 51-68.

[23] Shklover, V. ; Haibach, T.; Ried, F.; Nesper, R.; Novk, P.; Crystal Structure of the Product of Mg^{2+} Insertion into V_2O_5 Single Crystals. *J. Solid State Chem.* **1996** 123, 317-323.

[24] Millet, P.; Satto, C.; Bonvoisin, J.; Normand, B.; Penc, K.; Albrecht, M.; Mila, F.; Magnetic properties of the coupled ladder system MgV_2O_5. *Phys. Rev. B* **1998**, 57, 5005

[25] Millet, P.; Satto, C.; Sciau, P.; Galy J.; MgV_2O_5 and δ-$Li_xV_2O_5$ A Comparative Structural Investigation. *J. Solid State Chem.* **1998**, 136, 56-62.

[26] Zhou, B.; He, D.; Raman spectrum of vanadium pentoxide from density-functional perturbation theory *J. Raman Spectrosc.* **2008**, 39, 1475-1481.

[27] Splitaler, J.; Sherman, E. Y.; Ambrosch-Draxl, C.; First-principles study of phonons, optical properties, and Raman spectra in MgV_2O_5. *Phys. Rev. B* **2008**, 78, 064304

[28] Pereira-Ramos, J . P.; Messina R.; Perichon J.; Electrochemical formation of a magnesium vanadium bronze $Mg_xV_2O_5$ in sulfone-based electrolytes at 150°C. *J. Electroanal. Chem.* **1987**,218, 241-249

[29] http://en.wikipedia.org/wiki/Color

[30] Beckstein, O.; Klepeis, J. E.; Hart, G. L. W.; Pankratov, O.; First-principles elastic constants and electronic structure of α-Pt_2Si and PtSi. *Phys. Rev. B* **2001**, 63, 134112

[31] Ma, W. Y.; Zhou, B.; Wang, J. F.; Zhang X. D.; Jiang, Z. Y.; Effect of oxygen vacancy on Li-ion diffusion in a V_2O_5 cathode: a first-principles study. *J. Phys. D: Appl. Phys.* **2013**, 46, 105306

[32] Sheppard, D.; Xiao, P.; Chemelewski, W.; Johnson D. D.; Henkelman G.; A generalized solid-state nudged elastic band method. *J. Chem. Phys.* **2012**, 136, 074103-

The barrierless α and δ phase transformation is proposed as a possible explanation to the fully reversibility of the Mg battery with V_2O_5 cathode.